

# Concatenation of Space-Time Block Codes and Turbo Trellis Coded Modulation (ST-TTCM) Over Rician Fading Channels With Imperfect Phase Reference

Osman N. UCAN

Istanbul University Engineering Faculty, Electronics Dept.  
34850, Avcilar, Istanbul-Turkey

e-mail: uosman@istanbul.edu.tr

## ABSTRACT

*In this paper, the performance of Space-Time - Turbo Trellis Coded Modulation (ST-TTCM) is evaluated over Rician fading channels with imperfect phase reference. For high data transmission over wireless fading channels, Space-Time Block Codes provide the maximal possible diversity advantage for multiple decoding algorithms. The combined effects of fading channel and non-ideal coherent receiver on the phase of the received amplitude and of a noisy carrier reference are considered, each modeled by Rician and Tikhonov distributions respectively. Here, we investigate Space Time-Turbo Trellis Coded Modulation (ST-TTCM) for 8PSK for several Rician parameters  $K$  and effective signal-to-noise ratio in the carrier tracking loop  $\alpha$ . Thus, our results will reflect the degradations both due to the effects of the fading on the amplitude of the received signal and of a noisy carrier reference.*

**Key Words:** Turbo Trellis Coded Modulation, Space-Time Codes, Imperfect Phase Reference

## 1. INTRODUCTION

Turbo codes are the most efficient codes for low-power applications such as deep-space and satellite communications, as well as for interference limited applications such as third generation cellular and personal communication services. Since Turbo codes use convolutional codes as their constituent codes, a natural extension of the Turbo concept, which improves bandwidth efficiency is its application to systems using TCM. As in [1], the main principle of turbo codes is applied to TCM by retaining the important properties and advantages of both of their structures. Just as binary turbo codes use a

parallel concatenation of two binary recursive convolutional encoders, we have concatenated two recursive TCM encoders as in [2][3], and adapted the interleaving and puncturing.

Increasing the quality or reducing the effective error rate in a multipath fading channel is extremely difficult. In Additive White Gaussian Noise (AWGN), using typical modulation and coding schemes, reducing the effective bit error rate from  $10^{-2}$  to  $10^{-3}$  may require only 1 or 2 dB higher signal-to-noise ratio. Achieving the same in a multipath fading environment may require up to 10 dB improvement in SNR [6].

The improvement in SNR may not be achieved by higher transmit power or additional bandwidth, as it is contrary to the requirements of next generation systems. It is there for crucial to effectively reduce the effect of fading at both the remote units and the base stations, without additional power or any sacrifice in bandwidth.

Recently different transmit diversity techniques have been introduced to benefit from antenna diversity also in the downlink while putting the diversity burden on the base station. In [4] space-time trellis coding has been introduced proposing joint design of coding, modulation, transmit diversity and optimal receive diversity. Substantial benefits have been shown to be achieved by channel coding techniques appropriate to multiple transmit antenna systems. In this paper, we give a generalized scheme for concatenation of Space-Time block codes and Turbo Trellis Coded Modulation. Here the channel is Rician fading channel and there is an effective signal-to-noise ratio in the carrier tracking loop that results jitter effect. In the decoder side, symbol-by-symbol log-map algorithm and for the inputs of the decoder, channel estimator and combiner have been taken under consideration.

This paper is organized as: in Section 2, Space Time Block Codes scheme is explained, in Section 3, the over all system, Space Time-Turbo Trellis Coded Modulation (ST-TTCM) is given and in Section 4, ST-TTCM is simulated for different Rician fading parameters of our system. It is shown that there causes degradation due to SNR and effective signal-to-noise ratio in the carrier tracking loop  $\alpha$ .

## 2. SYSTEM MODEL

In this Section, we investigate Space Time-Turbo Trellis Coded Modulation (ST-TTCM) over fading channel. The general block diagram of the considered scheme is given in Figure 1. Here, the main emphasis is on the performance of the ST-TTCM in fading environment modeled by Rician probability density function. The combined effects of fading and the non-ideal coherent receiver on the phase of the received signal are taken into account. Thus our results reflect the degradations both due the effects of fading on the amplitude of the received signal and of a noisy carrier reference.

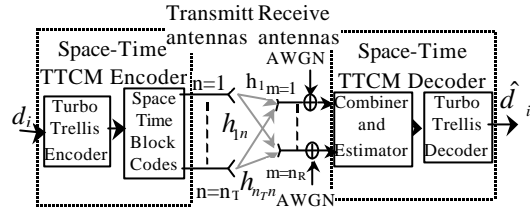


**Figure 1.** General Block Diagram of (ST-TTCM)

The input binary data is passed through a turbo encoder followed by a Space-Time block encoder which is shown in Figure 2. Furthermore at the transmitter side,  $n_T$  number of antennas are placed in order to achieve delay diversity and the Figure 3 shows the space-time block codes. The channel is modeled as Rician fading with imperfect phase reference. The amplitude and phase distortion of the channel is carried out by  $h$  parameters shown in Figure 4. At the receiver side, the distorted multi-path signals arrive to at  $n_R$  number of receiver antennas. At the decoder of ST-TTCM scheme, turbo-trellis decoder follows combiner and estimator. Then  $\hat{d}_i$  data sequence is estimated.

### 2.1 Space-Time Block Codes

In wireless communication, multipath fading results severe amplitude and phase distortion. So it is crucial to combat the effect of the fading at both the remote units and the base stations, without additional power or any sacrifice in bandwidth. Since the transmitter has no information about the channel fading characteristics, it has to be fed from the receiver to the transmitter, which results complexity to both transmitter and receiver. In some cases, there may be no link in between them. There are some effective techniques, which are time and frequency diversity. Time interleaving may result in large delays.

Spread spectrum approaches are ineffective if the coherent bandwidth of the channel is larger than the spreading bandwidth. So we can conclude that in fading environments, antenna diversity is a practical, effective and, hence a widely used technique for reducing the effect of multipath fading [5][6]. Space-time coding is a bandwidth and power efficient method of communication over Rician fading channels that realizes the benefits of multiple transmit antenna [4].

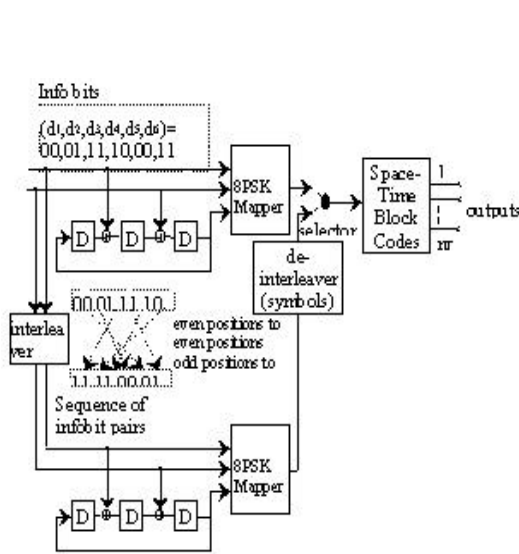


Figure 2. Encoder of ST-TTCM for 8PSK

Figure 3 shows an example for a space-time block encoder. Input of a Space-Time block encoder is a block of  $K$  complex  $x_i, i=1...K$ , where  $x_i$  are elements of a higher order modulation constellation, e.g. M-PSK. The space-time block encoder maps the input symbols on entries of a  $p \times n_T$  matrix  $G$ , where  $n_T$  is the number of transmit antennas. The entries of the matrix  $G$  are the  $K$  complex symbol  $x_i$ , their complex conjugate  $x_i^*$  and linear combinations of  $x_i$  and  $x_i^*$ . The  $p \times n_T$  matrix  $G$  which defines the Space-Time Block Code is a complex generalized orthogonal as defined [5], which means that the columns of  $G$  are orthogonal. An examples for  $n_T = 2$  is the complex generalized orthogonal design

$$G_1 = \begin{bmatrix} g_{11} & \Lambda & g_{1n_T} \\ M & & M \\ g_{p1} & \Lambda & g_{pn_T} \end{bmatrix} = \begin{bmatrix} x_1 & x_2 \\ -x_2^* & x_1^* \end{bmatrix} \quad (1)$$

In this paper, we consider a simple transmit diversity scheme which improves the signal by simple processing across two transmitter antennas and one receiver antenna as shown in Figure 4. We assume ST-TTCM modulated two signals are simultaneously sent from the two transmitter antennas,  $tx_o, tx_1$ . In the first coding step, the signal transmitted

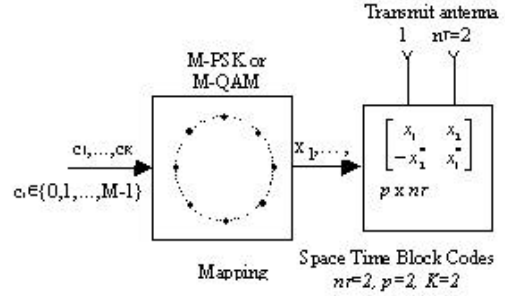


Figure 3. Space Time Block Code Encoder

from the first antenna,  $tx_o$  is denoted as  $s_o$  and from the second antenna  $tx_1$  as  $s_1$ . In the second coding step; antenna  $tx_o$ , transmits  $(-s_1^*)$ , while antenna  $tx_1$ , transmits  $s_o^*$  where  $*$  means complex conjugate operation. Let assume that Rician channel with imperfect phase reference fading is constant during these two consecutive symbols. The Rician channel in between the transmitter antenna,  $tx_o$  and receiver antenna is defined as  $h_o$ . The channel between the transmitter antenna,  $tx_1$  and the receiver is defined as  $h_1$ . The multipath channels  $h_o$  and  $h_1$  are modelled as,

$$h_o(t) = h_o(t+T) = \mathbf{r}_o e^{j\mathbf{q}t} \\ h_1(t) = h_1(t+T) = \mathbf{r}_1 e^{j\mathbf{q}t} \quad (2)$$

where  $T$  is the symbol duration.  $\mathbf{r}$  is fading amplitude and the term  $e^{j\mathbf{q}}$  is a unit vector where  $\mathbf{q}$  represents the phase noise as mentioned in [9,10], which is assumed to have Tikhonov pdf given by,

$$p(\mathbf{q}) = \frac{e^{-\alpha \cos \mathbf{q}}}{2\alpha I_0(\alpha)} \quad |\mathbf{q}| \leq \pi \quad (3)$$

where  $I_0$  is the modified Bessel function of the first kind order zero and  $\alpha$  is effective signal-to-noise ratio in the carrier tracking loop.

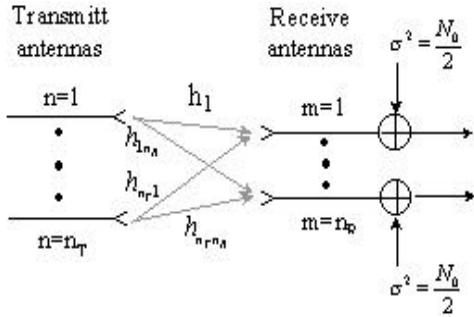


Figure 4. Space-Time Antenna Configuration

In this paper, we investigate bit error performance of ST-TTCM over Rician environment without Channel State Information (CSI) [7][8]. Rician probability density function can be written as,

$$P(r) = 2r(1+K) e^{(-r^2(1+K)-K)} I_0 [2r\sqrt{K(1+K)}] \quad (4)$$

K is fading parameter. The received signals can be expressed as [6],

$$\begin{aligned} r_o &= r(t) = h_o s_o + h_1 s_1 + n_o \\ r_1 &= r(t+T) = -h_o^* s_1 + h_1^* s_o + n_1 \end{aligned} \quad (5)$$

where  $r_o$  and  $r_1$  are received signals at time  $t$  and  $t+T$  and  $n_o$  and  $n_1$  are Gaussian Noise with the noise variance is  $\sigma^2 = \frac{N_o}{2E_s}$ .

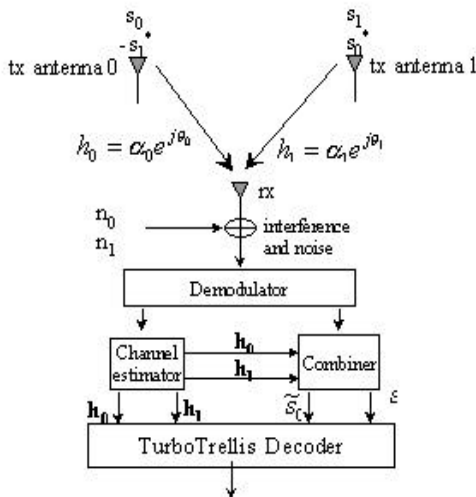


Figure 5. Receiver Side Block Diagram of ST-TTCM

The combiner in Figure 5, forms the following signals which are fed to ST-TTCM decoder.

$$\begin{aligned} s_o &\approx h_o^* r_o + h_1 r_1^* \\ s_1 &\approx h_1^* r_o - h_o r_1^* \end{aligned} \quad (6)$$

Substituting Equations (2) and (5), we get,

$$\begin{aligned} s_o &\approx (\mathbf{r}^2_o + \mathbf{r}^2_1) s_o + h_o^* n_o + h_1 n_1^* \\ s_1 &\approx (\mathbf{r}^2_o + \mathbf{r}^2_1) s_1 - h_o n_o^* + h_1^* n_1 \end{aligned} \quad (7)$$

The output of Equation (7) are now entries of our Turbo Trellis decoder (Figure 6).

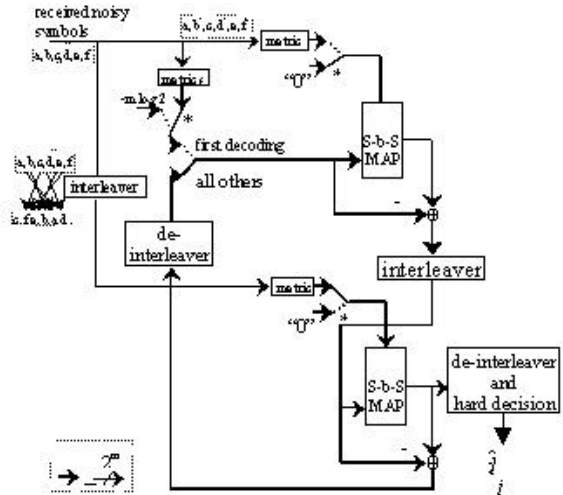


Figure 6. Decoder of ST-TTCM for 8PSK

### 3. SPACE-TIME - TURBO TRELLIS CODED MODULATION SCHEME

In this Section, we investigate the performance of Space-Time - Turbo Trellis Coded Modulation (ST-TTCM) over AWGN and Rician channels and assume that phase distortion is also available. The block diagram of the ST-TTCM system operating over imperfect phase reference and various fading environments are shown in Figure 1. We present Space Time Block Codes for Turbo Trellis Coded signals. Space Time coding achieves higher error performance without increasing bandwidth by using various combinations of antennas diversity. As we know

Turbo Trellis Coded Modulation (TTCM) is similar to binary turbo codes, but employs Trellis Coded Modulation (TCM) codes which include multi-dimensional codes. The combination of turbo codes with trellis codes leads to a straightforward encoder structure, and allows iterative decoding as binary turbo decoder. However, iterative Turbo Decoder needs to be adapted to the decoding of TCM codes. Here, we investigate ST-TTCM for 8PSK for several Rician parameters  $K$  and effective signal-to-noise ratio in the carrier tracking loop  $\alpha$ . Thus, our results will reflect the degradations both due to the effects of the fading on the amplitude of the received signal and of a noisy carrier reference.

### 3.1 ST-TTCM Encoder

Turbo codes use convolutional codes as their constituent codes, a natural extension of the Turbo concept, which improves bandwidth efficiency is its application to systems using TCM. As in [2][3], the main principle of turbo codes is applied to TCM by retaining the important properties and advantages of both of their structures. Essentially, TCM codes can be seen as systematic feedback convolutional codes followed by one (or more for multi dimensional codes) signal mapper(s). Just as binary turbo codes use a parallel concatenation of two binary recursive convolutional encoders, we have concatenated two recursive TCM encoders as in [2], and adapted the interleaving and puncturing.

The most important characteristic of turbo codes is their simple use of recursive systematic component codes in a parallel concatenation scheme. Pseudo-random bit-wise interleaving between encoders ensures a small bit-error probability [4]. In [2], Ungerboeck codes (and multidimensional TCM codes) have been employed as building blocks in a Turbo Coding scheme in a similar way as binary codes were used.

We use the encoder which is shown in Figure 2 and introduced in [2] and [3], and we will not give any more detail for this known structure.

### 3.2 ST-TTCM Decoder

The Turbo Trellis Decoder is similar to that used to decode binary turbo codes, except there is a difference passed from one decoder to the other, and the treatment of the very first decoding step.

In binary turbo coding, the decoder's output can be split into three parts. These parts are systematic component, a priori component, and extrinsic component [10]. But only the extrinsic component may be given to the next decoder; otherwise, information will be used more than once in the next decoder [1].

Here, for the Turbo Trellis Decoder the systematic information is transmitted together with parity information in the same symbol. However, we can split the decoder output into two different components, first one is a priori and the second is extrinsic and systematic together.

#### 3.2.1 Metric Calculation

Matrix calculation was used in the very first decoding stage as in [2]. We have relied on the fact that if the upper decoder sees a group of  $n$  punctured symbols, we have embedded the systematic information in the a priori input (Figure 6). Before the first decoding pass off the upper decoder, we need to set the a priori information to contain the systematic information for the  $*$  transitions, where the symbol is transmitted partly by the information group  $d_k$ , but also the unknown parity bit  $b_k^{0,*} \in \{0,1\}$  produced by the other encoder. We set the a priori information, by applying the mixed Bayes' rule, to

$$\begin{aligned} \Pr\{d_k = i | y_k\} &= \text{const} \cdot p(\mathbf{y}_k | d_k = i) \\ &= \text{const} \cdot \sum_{j \in \{0,1\}} p(\mathbf{y}_k, b_k^{0,*} = j | d_k = i) \\ &= \frac{\text{const}}{2} \cdot \sum_{j \in \{0,1\}} p(\mathbf{y}_k | d_k = i, b_k^{0,*} = j) \end{aligned} \quad (8)$$

where it is assumed that  $\Pr\{b_k^{0,*} = j | d_k = i\} = \Pr\{b_k^{0,*} = j\} = 1/2$  and  $\mathbf{y}_k = (y_k^0, \dots, y_k^{(n-1)})$  if the receiver observes  $N$  set of  $n$  noisy symbols, where  $n$  such symbols are associated with each step in the trellis. In Equation 8, it is not necessary to calculate the value of the constant since the value of  $\Pr\{d_k = i | \mathbf{y}_k\}$  can be determined by dividing the summation  $\sum_{j \in \{0,1\}}$  by its sum over all  $i$  (normalization). If the upper decoder is not at the a  $*$  transition, then we set  $\Pr\{d_k = i\} = 1/2^m$  where  $m$  is the number of Turbo Trellis encoder input.

To illustrate the performance in the log domain, consider the *Jacobian Logarithm*:

$$\begin{aligned} \ln(e^x + e^y) &= \max(x, y) + \ln(1 + \exp\{-|y-x|\}) \\ &= \max(x, y) + f_c(|x-y|) \end{aligned} \quad (9)$$

First of all the state transitions must be calculated by the given formulation below,

$$\begin{aligned} \mathbf{g}(y_k, M', M) &= p(y_k | d_k = i, S_k = M, S_{k-1} = M') \\ &\cdot q(d_k = i | S_k = M, S_{k-1} = M') \\ &\cdot \Pr\{S_k = M | S_{k-1} = M'\} \end{aligned} \quad (10)$$

$q(d_k = i | S_k = M, S_{k-1} = M')$  is either zero or one, depending on whether encoder input  $i \in \{0, 1, \dots, 2^m - 1\}$  is associated with the transition from state  $S_{k-1} = M'$  to  $S_k = M$  or not. In the last component of Equation 10, we use the a priori information

$$\begin{aligned} \Pr\{S_k = M | S_{k-1} = M'\} \\ = \begin{cases} \Pr\{d_k = 0\}, & \text{if } q(d_k = 0 | S_k = M, S_{k-1} = M') = 1 \\ \Pr\{d_k = 1\}, & \text{if } q(d_k = 1 | S_k = M, S_{k-1} = M') = 1 \\ \Pr\{d_k = 2^m - 1\}, & \text{if } q(d_k = 2^m - 1 | S_k = M, S_{k-1} = M') = 1 \\ = \Pr\{d_k = j\} \end{cases} \end{aligned} \quad (11)$$

where  $j: q(d_k = j | S_k = M, S_{k-1} = M') = 1$ . If there does not exist a  $j$  such that  $q(d_k = j | S_k = M, S_{k-1} = M') = 1$ , then  $\Pr\{S_k = M | S_{k-1} = M'\}$  is set to zero

Now let  $\bar{\mathbf{g}}_i(s_k \rightarrow s_{k+1})$  be the natural logarithm of  $\mathbf{g}_i(s_k \rightarrow s_{k+1})$

$$\bar{\mathbf{g}}_i(s_k \rightarrow s_{k+1}) = \ln \mathbf{g}_i(s_k \rightarrow s_{k+1}) \quad (12)$$

Now let  $\bar{\mathbf{a}}(s_k)$  be the natural logarithm

of  $\mathbf{a}(s_k)$ ,

$$\begin{aligned} \bar{\mathbf{a}}(s_k) &= \ln \mathbf{a}(s_k) \\ &= \ln \left\{ \sum_{s_{k-1} \in A} \exp [\bar{\mathbf{a}}(s_{k-1}) + \bar{\mathbf{g}}(s_{k-1} \rightarrow s_k)] \right\} \end{aligned} \quad (13)$$

where  $A$  is the set of states  $s_{k-1}$  that are connected to the state  $s_k$ .

Now let  $\bar{\mathbf{b}}(s_k)$  be the natural logarithm of  $\mathbf{b}(s_k)$ ,

$$\begin{aligned} \bar{\mathbf{b}}(s_k) &= \ln \mathbf{b}(s_k) \\ &= \ln \left\{ \sum_{s_{k+1} \in B} \exp [\bar{\mathbf{b}}(s_{k+1}) + \bar{\mathbf{g}}_i(s_k \rightarrow s_{k+1})] \right\} \end{aligned} \quad (14)$$

where  $B$  is the set of states  $s_{k+1}$  that are connected to state  $s_k$ . Therefore, the desired output of the MAP decoder is

$$\begin{aligned} P_i\{d_k = i | \mathbf{y}\} &= \\ \text{const} \sum_M \sum_{M'} & \left[ \bar{\mathbf{g}}(y_k, M', M) + \bar{\mathbf{a}}_{k-1}(M') + \bar{\mathbf{b}}_k(M) \right] \end{aligned} \quad (15)$$

$\forall i \in \{0, \dots, 2^m - 1\}$ . The constant can be alimanted by normalizing the sum of above formulation over all  $i$  to unity.

## 4. SIMULATION RESULTS

In the encoder structure as shown in Figure 2, we have two information inputs, each with 1024 bit frame size. To create parity bits, both encoders are constituted of three memories. 8PSK mappers were used, and Space-Time block has been located after the puncturer. At the decoder, the signals reach to the receiver antenna from the two transmitter antennas using multipath fading environment (Figure 4 and 5). Quadrature and inphase coordinates of the received noisy signal is detected by using the noisy phase value. Then they are processed by Space-Time decoder with channel estimator and combiner blocks. The pre-processed noisy signals are evaluated by Turbo-Trellis Decoder as shown in Figure 6. As an example, we simulate ST-TTCM system for 8PSK over AWGN and Rician channel with imperfect noise reference. We obtain the simulation curves for different  $K$ ,  $\alpha$  and SNR values. Although Space-Time Block Codes provide up to 10dB improvement over Rayleigh (or  $K=0$  for Rician) channel in SNR. All the simulation results were obtained for Rician fading channel. The Figure 7a, shows the performance of ST-TTCM signals for  $K=\infty$  with ideal phase reference. It is shown that as  $K$  tends to AWGN, bit error performance improves. The Figure 7b, gives the performance curves for  $K=\infty$  dB with non-ideal phase references of  $\alpha = 20$  dB values. In Figure 7c, performance is simulated for  $K=\infty$  and  $\alpha=10$  dB. And Figure 8a, shows the performance of TTCM signals for  $K=10$  dB with ideal phase reference. The Figure 8b, gives the performance curves for  $K=10$  dB with  $\alpha = 20$  dB values. The Figure 8c, gives the performance curves for  $K=10$  dB with non-ideal phase references of  $\alpha = 10$  dB. The Figure 9a, gives the performance curves for  $K=0$  dB with non-ideal phase references of  $\alpha = \infty$ . The Figure 9b, gives the performance curves for  $K=0$  dB with non-ideal phase references of  $\alpha = 20$  dB values. The Figure 9c, gives the performance curves for  $K=0$  dB with non-ideal phase references of  $\alpha = 10$  dB values. It is clear that for a constant iteration number, as  $K$  increases, performance improves for the same SNR values. To emphasize the importance of imperfect phase effect, the performance of the considered scheme is simulated with various  $\alpha$  and  $K$  values. For  $\alpha = 10, 20, \infty$  dB and  $K=0, 10, \infty$  SNR value, as iteration number increases, performance gets better. It is clear that phase jitter distortion is effective for Rician fading.

When the performance results obtained in Figure 7 through Figure 9 are compared, the degradation of error performance due to phase distortion can easily be seen for all SNR and K values.

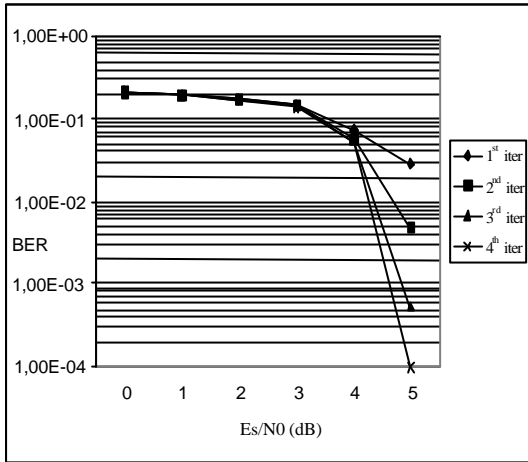


Figure 7a. Bit error performance of 8PSK ST-TTCM for  $K=\infty$ , without phase jitter

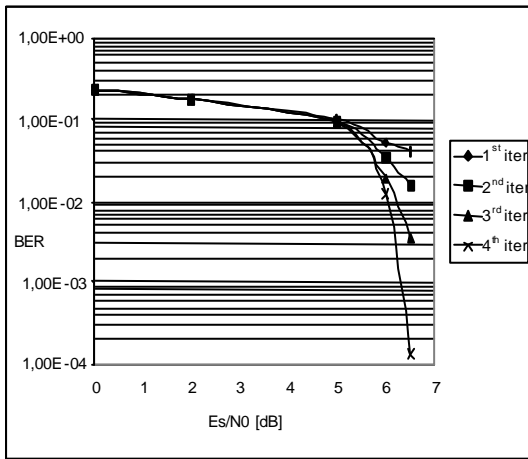


Figure 7b. Bit error performance of 8PSK ST-TTCM for  $K=\infty$ , jitter effect  $\alpha=20$  dB

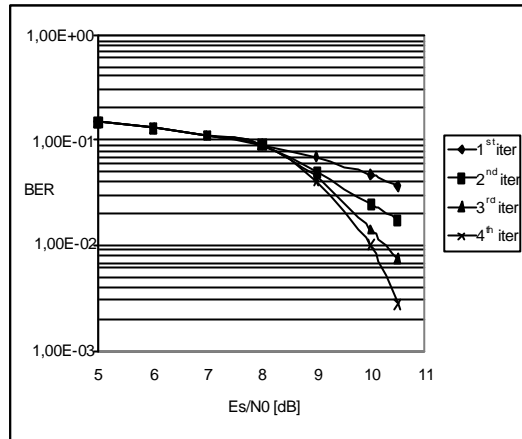


Figure 7c. Bit error performance of 8PSK ST-TTCM for  $K=\infty$ , jitter effect  $\alpha=10$  dB

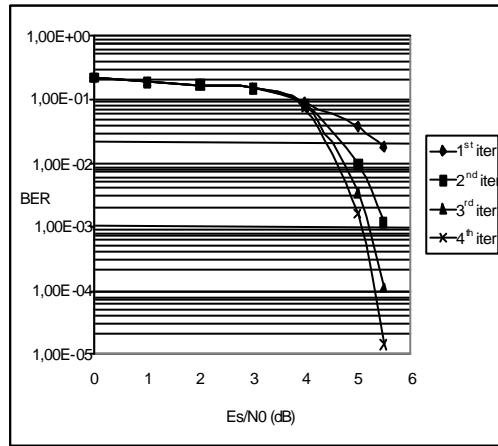


Figure 8a. Bit error performance of 8PSK ST-TTCM for  $K=10$  dB,  $\alpha=\infty$  dB

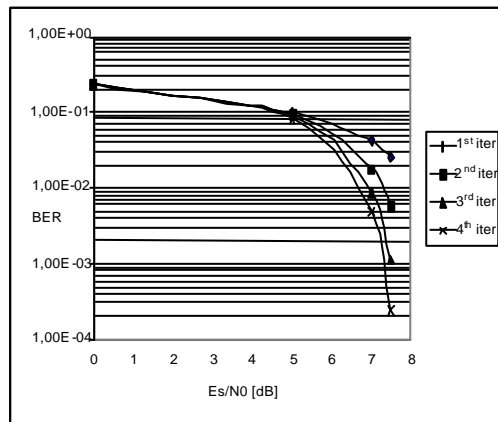


Figure 8b. Bit error performance of 8PSK ST-TTCM for  $K=10$  dB,  $\alpha=20$  dB

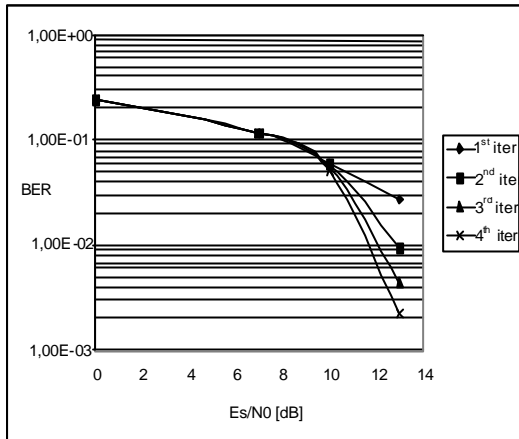


Figure 8c. Bit error performance of 8PSK ST-TTCM for  $K=10\text{dB}$ ,  $\alpha=10\text{ dB}$

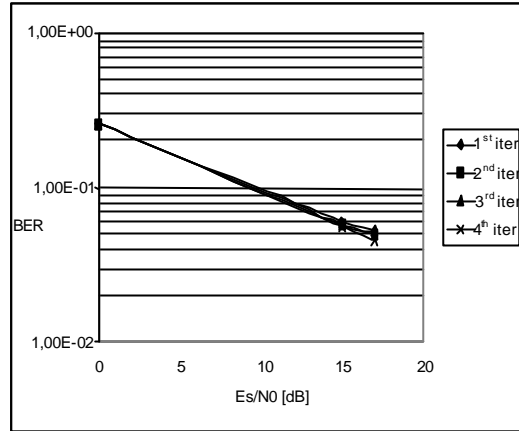


Figure 9c. Bit error performance of 8PSK ST-TTCM for  $K=0\text{dB}$ ,  $\alpha=10\text{ dB}$

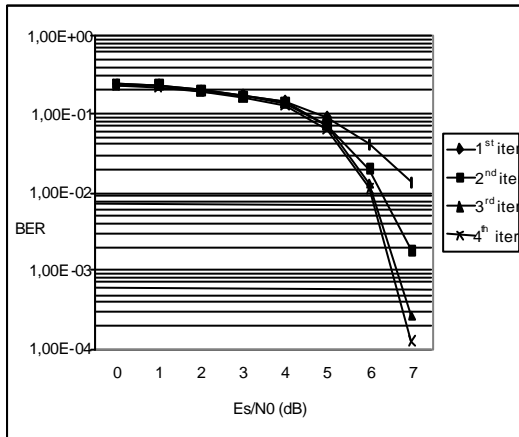


Figure 9a. Bit error performance of 8PSK ST-TTCM for  $K=0\text{dB}$ ,  $\alpha=\infty\text{ dB}$

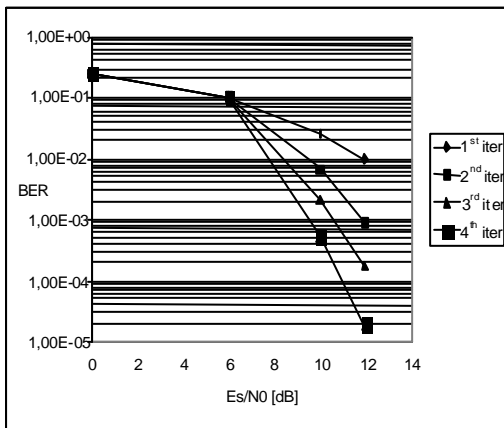


Figure 9b. Bit error performance of 8PSK ST-TTCM for  $K=0\text{dB}$ ,  $\alpha=20\text{ dB}$

### 5. CONCLUSION

We know the importance of antenna diversity using especially for deep space and satellite communications, as well as for interference limited applications such as third generation cellular and personal communication services because of the bandwidth problem. In this paper we have shown performance of space time-turbo trellis codes over Rician fading channels with jitter effect. As an example, the jitter performance of turbo trellis coded modulated signals are simulated with different fading parameter  $K$ , effective signal-to-noise ratio in the carrier tracking loop  $\alpha$ , iteration number and data block size  $N$ .

### 6. REFERENCES

- [1].Berrou C, Glavieux A, Thitimasjshima P. "Near Shannon-limit error correcting coding and decoding: Turbo codes (1)", *IEEE International Conference on Communication*,; 1064-1070, Geneva Switzerland May 1993.
- [2].Robertson P, Worzt T. "Bandwidth-efficient Turbo Trellis-coded modulation using punctured component codes", *IEEE J. SAC*, Vol. 16, February 1998.
- [3].Blackert W, Wilson S. "Turbo Trellis Coded Modulation", *Conference Information Signals and System CISS*, 1996.
- [4].Alamouti SM. "A Simple Transmit Diversity Technique for Wireless Communication", *IEEE Journal of Selected Areas in Communication*, 16(8), October 1998.
- [5].Tarokh V, Seshadri N, Calderbank A. "Space-time codes for high data rate wireless



communication: Performance criterion and code construction”, *IEEE Transaction on Information Theory*, 44:744-765, March 1998.

[6].Tarokh V, Jafarkhani H, Calderbank A. “Space-time codes from orthogonal design”, *IEEE Transaction on Information Theory*, June 1999.

[7].Ucan O.N, Osman O, Gumus A. “Performance of Turbo coded signals over partial response fading channels with imperfect phase reference”, *IEEE 43. Midwest Symposium on Circuits and Systems MWSCAS*, 04000-25, Michigan, 2000.

[8].Ucan ON. “Trellis coded quantization /modulation over mobile satellite channel with imperfect phase reference”, *International Journal of Satellite Communications*, 16:169-175, 1998.

[9].Divsalar D, Simon MK. “The design of trellis coded MPSK for fading channels: Performance criteria”, *IEEE Transaction On Communication*, 36:1004-1012, 1998.

[10]. Ucan O N, Osman O, Paker S. “Turbo Coded Signals over Wireless Local Loop Environment”, *AEU* (accepted).

### Authors' Biography



**Osman Nuri Uçan** was born in Kars on January, 1960. He received the B.S.E.E., M.S.E.E. and PhD. degrees in Electronics and Communication Engineering Department from the Istanbul Technical University (ITU) in 1985, 1988 and 1995 respectively. During 1986-1997 he worked as a research assistant in the same university. In 1996 he became technical coordinator at an important Turkish firm. He also worked as supervisor at TUBITAK-Marmara Research Center in 1998. He is now associate Professor and Vice President of Electrical&Electronics Engineering Department of Istanbul University (IU). He is computer network director of Avcilar campus of IU and co-coordinator of "Construction Organisation" of IU. He is organization committee member of "IEEE Signal Processing and Applications Conference (SIU)" and chief editor of "Recent Researches on Electronics and Earth Science Conference (RREESC)" to be held in 2001. He is member of "Publications and Science Committee" of IU.

His current research areas include: information theory, jitter analysis of modulated signals, channel modelling, cellular neural network systems, random neural networks, wavelet, turbo coding and Markov Random Fields applications on real geophysics data, satellite based 2-D data and underwater image processing.

In his studies, he has defined quadrature partial response-trellis coded modulation (QPR-TCM), Uçan receivers, Osman Nuri Uçan decoders, effective code memory, partial response fading channel, partial response microwave channel, combined trellis coded quantization/modulation (C TCQ/TCM), segmented cellular neural network –cellular neural network combined trellis coded quantization/ modulation (SCNN-CNN CTCQ/TCM), Differential Cellular Neural Network (DCNN), Differential Markov Random Field (DMRF), Cellular Random Neural Network (CRNN).

He is the supervisor of 7 PhD. , 9 Master degree and 39 graduate students of various universities of Turkey. He is married and has one son and one daughter.